Submitted: 13 November, 2024 Accepted: 08 January, 2025 Published: 03 May, 2025 DOI:10.22514/jocpd.2025.062

ORIGINAL RESEARCH

Journal of Clinical Pediatric Dentistry

Upper airway dimensions with different skeletal malocclusions? A cross-sectional study in Vietnamese children

Lam Nguyen Le[1,*], Trinh Thi Ngoc Nguyen[2], Loc Truong Tan[2], Tranh Thi Huyen Trinh[2], Phung Thi Thanh Nguyen[2], Khanh Vu Phuong Le[2]

[1]Department of Pediatrics Dentistry and Orthodontics, Faculty Odonto-Stomatology, Can Tho University of Medicine and Pharmacy, 700000 Can Tho, Vietnam
[2]Faculty Odonto-Stomatology, Can Tho University of Medicine and Pharmacy, 700000 Can Tho, Vietnam

***Correspondence**
lenguyenlam@ctump.edu.vn
(Lam Nguyen Le)

Abstract

Background: This study aimed to evaluate the effect of craniofacial structure on maxillary airway morphology with skeletal Class I, II and III malocclusions using lateral cephalometric radiographs and cone beam computed tomography (CBCT) in Vietnamese children. **Methods**: This was a cross-sectional study conducted between June 2023 and June 2024. Study participants included 105 children (14–18 years old, 50 males and 55 females) with a body mass index of 18–25 kg/m^2, no history of orthodontic treatment or orthognathic surgery, and no history of cleft lip or palate treatments. Lateral cephalometric radiographs and CBCT were used to identify differences in airway dimensions and respiratory function and assess correlations between craniofacial structure and maxilla airway morphology. **Results**: The study found a decrease in mandibular length in skeletal groups with CI CII and CIII malocclusion, but significant differences were observed between skeletal CI and CII and between skeletal CII and skeletal CIII. CIII had the largest airway width, followed by CI and CII. The pharyngeal airway volume on CBCT radiographs showed a negative relationship between airway parameters on lateral cephalometric radiographs and airway volume on CBCT radiographs. The Angle formed by the A-nasion line and B-nasion line (ANB) and angle formed by the SN line and GoGn line (SN-GoGn) angles, the angle between the Frankfort plane and mandibular plane (FMA) and the Y-axis showed a positive correlation with mandibular body length, the facial axis and the facial angle. There was also a positive correlation between airway parameters on lateral cephalometric radiographs and airway volume on CBCT radiographs. **Conclusions**: There was a strong correlation between airway volume and skeletal patterns. Airway dimensions were significantly reduced in skeletal Class II malocclusion patients with a high ANB angle, retrognathic mandible and vertical growth pattern. Clinicians should exercise caution when performing mandibular retrusion in skeletal Class II patients to avoid worsening airway obstruction.

Keywords

Airway obstruction; Cone beam computed tomography; Lateral cephalometry; Malocclusion; Vietnamese population

1. Introduction

Radiography is an indispensable tool in orthodontic practice [1, 2]. The primary function of lateral cephalometric reference lines is to describe and classify craniofacial structures and dentition. The most commonly used reference planes are the Frankfort horizontal (FH) plane, which is defined as a line drawn between the inferior orbital rim and the supratragic notch, and the anterior cranial base plane (SN plane), a horizontal plane passing through the sella turcica and nasion and represents the anterior cranial base [3]. However, two-dimensional imaging techniques are ineffective in accurately reconstructing three-dimensional (3D) structures and their related pathologies [1, 4]. However, cone beam computed tomography (CBCT) has enabled the accurate estimation of craniofacial bone volume and airway dimensions. It also facilitates evaluating the effects of various orthodontic or orthopedic treatments on airway volume, including the advancement of the mandible and the expansion of the maxilla [5–8].

Recently, the relationship between respiratory function and craniofacial morphology has garnered increasing attention [1]. Previous studies have indicated a relationship between the maxillary airway and facial development [1, 9, 10]. The maxillary airway is a complex structure comprising bones, cartilage and soft tissues that adapt to functions related to

respiration, swallowing and phonation. The effect of breathing patterns on facial development became a focal point for the orthodontic community in the 1970s. Mouth breathing, as opposed to nasal breathing, can negatively affect growth and development, leading to a tendency for mandibular positioning of the mandible and tongue and altering the growth direction of craniofacial structures [9].

Dodda *et al*. [11] used lateral cephalometric radiographs to describe the distinctive characteristics of Class II, Division 2 malocclusion, as classified by angles while Di Carlo *et al*. [9] studied the maxillary airway's morphology and dimensions through 3D radiological measurements in 90 young adult patients. In the latter study, the sagittal plane was assessed, and patients were divided into three groups according to the value of the ANB angle. In another study, Sfondrini *et al*. [12] evaluated the maxillary airway in adult Caucasian subjects without previous orthodontic treatment. Their main objective was to measure the maxillary airway dimensions in adult skeletal Class I, II and III patients. Pop *et al*. [1] recently evaluated several parameters, including the morphology and volume of the maxillary airway in relation to angle Class I, II and III occlusions. That study concluded that the narrowest segment of the pharynx had the highest value in patients with angle Class III malocclusions. Furthermore, the volume of the oropharynx was found to be greater in angle Class III compared to Class II patients. However, these studies did not compare measurements obtained using two different diagnostic methods: lateral cephalometric radiographs and CBCT.

A 2022 review evaluated the scientific evidence concerning the effect of various orthodontic treatment modalities on the airway. The review highlighted the significant role of orthodontists in recognizing respiratory issues in patients and correlating these with malocclusion patterns to determine appropriate treatment strategies [13, 14]. Rodrigues *et al*. [15] (2024) demonstrated a significant correlation between skeletal malocclusion classification and pharyngeal airway dimensions. Their study revealed that as skeletal malocclusion progresses toward a Class III pattern, there is a concomitant increase in the pharyngeal airway's volume and cross-sectional area. To this end, radiographic measurement techniques have gradually become standardized and indispensable tools in orthodontics as treatment goals and requirements have increased [16, 17]. In 1931, Broadbent (USA) and Holrath (Germany) introduced the standard cephalometric technique, which creates 1:1 images with the object being photographed. This technique, along with direct measurements on a model cast, has become an indispensable tool in diagnoses, treatments and research in the field of orthodontics [18, 19]. Specifically, evaluations using lateral cephalometric radiographs and CBCT have become crucial to accurate diagnoses [20]. However, few studies have been conducted in the Mekong Delta region of Vietnam that provide an overview of the distribution and characteristics of malocclusion. Therefore, this study aimed to evaluate the effect of craniofacial structures on maxillary airway morphology in patients with skeletal Class I, II and III malocclusions using lateral cephalometric radiographs and CBCT in Vietnamese children.

2. Materials and methods

2.1 Study participants

Participants for the study were selected based on the following inclusion criteria: individuals who visited the Can Tho University of Medicine and Pharmacy Hospital, aged between 14 and 18 years, and with a body mass index (BMI) ranging from 18 to 25 kg/m^2. Exclusion criteria for the study included individuals with a history of orthodontic or orthognathic surgery, treatment for cleft lip or palate, or those whose dentition exhibited severe crowding. Additional exclusions applied to those with abnormal maxillary sagittal positioning, apparent maxillary dental arch stenosis, or a history of nasal cavity or sinus surgery. Participants reporting long-term nasal obstruction or who had experienced an acute maxillary respiratory tract infection within the two weeks prior to the study were also excluded [21, 22].

2.2 Study methods

This was a cross-sectional study conducted from June 2023 to June 2024 investigating 105 children (14–18 years old, 50 males and 55 females). Each participant underwent CBCT, and lateral cephalometric radiographs were taken to identify differences in airway dimensions and respiratory function and analyze the correlation between craniofacial structure and maxillary airway morphology (Table 1). The participants were divided into three groups based on their sagittal skeletal pattern: skeletal Class I (ANB angle between 0° and 4°), skeletal Class II (ANB angle $\geq$4°) and skeletal Class III (ANB angle $<$0°). The lateral cephalometric measurements, and the ANB, angle between the anterior cranial base plane (SN) plane and Steiner's mandibular plane (GnGo-SN), angle between the Frankfort (FH) plane and Downs' mandibular plane (Go-Me) (FMA), mandibular body length, the facial axis, the L1 to mandibular plane angle, PNS-AD2, SPAS and IAS were all significantly different between the three types of malocclusions (skeletal CI, CII and CIII). The Can Tho University of Medicine and Pharmacy's Research Ethics Committee approved the study (Approval number: No: 23.002/PCT-HDDD).

2.3 Study procedure

2.3.1 Scanning device

For imaging, patients were positioned upright, with a predefined head position, where the reference horizontal plane was established by the FH plane using a contour and digital gauge. Patients were instructed not to swallow or breathe during imaging. The radiographs were obtained using a Sirona Orthophos SL (Sirona, Germany), with a voxel base size of 0.08 mm, power lines and voltages of 3.0–16.0 mA and 60–90 kV, respectively, a scanning time of 14.9 seconds, and the capacity for cylindrical (field of view) measurements of 40–40 mm, 60–60 mm or 80–80 mm (according to the as low as reasonably achievable (ALARA) guidelines) [23].

TABLE 1. Measurement descriptions.

Variable	Definition
Volumes	
Nasopharynx (NP) (mm^3)	The region superior to the plane passes through the two points of the posterior nasal spine (PNS) on both sides and the first cervical vertebra (C1)
Oropharynx (OP) (mm^3)	The region inferior to the plane passes through the two points of the posterior nasal spine (PNS) on both sides and the first cervical vertebra (C1)
Total pharynx (TP) (mm^3)	The volume that includes both the nasopharynx and oropharynx
Distances	
PNS-AD1 (mm)	Distance measured from the most posterior point on the bony hard palate to the intersection of the PNS-(Basion) Ba line and the posterior nasopharyngeal wall
PNS-AD2 (mm)	Distance measured from the most posterior point on the bony hard palate to the intersection of the PNS-Hormion (H) line and the posterior nasopharyngeal wall
SPAS (mm)	The superior nasopharyngeal airway space
MAS (mm)	The middle oropharyngeal airway space
IAS (mm)	The inferior hypopharyngeal posterior airway space
Go-Me (mm)	Distance measured from the mental tubercle of the mandible to the angle of the mandible. In cases where the two halves of the mandible had not fused, the mental symphysis was used as a reference point
Lower Anterior Facial Height (LAFH) (mm)	Distance measured from the anterior nasal spine (ANS) to the Menton (Me)
Angles	
SNA (°)	Angle between the line Sella (S)-Nasion (N) and line Nasion (N)-point A. This angle measures the position of the maxilla relative to the skull base
SNB (°)	Angle between the line Sella (S)-Nasion (N) and line Nasion (N)-point B. This angle measures the mandibular's position relative to the skull base
ANB (°)	Angle between line A-the Nasion (N) and line B-Nasion (N), indicating the relationship between the maxilla and mandibular
SN-GoGn (°)	Angle between the anterior cranial base plane (SN) plane and Steiner's mandibular plane
FMA (°)	Angle between the Frankfort (FH) plane and Downs' mandibular plane (Go-Me)
Facial axis (°)	Angle between the Basion (Ba)-N line and the Pt-Gn line
Y-axis (°)	Angle between the S-Gn and FH planes
Facial Angle (°)	Angle between the FH plane and the N-Pog line
L1-MP (°)	Angle formed by the long axis of the mandibular incisor and the mandibular plane

ANS: anterior nasal spine; PNS: posterior nasal spine; FH: Frankfort horizontal; Me: Menton the most inferior point of the outline of the symphysis in the midsagittal plane; Hormion (H): the cephalometric point located near the adenoidal tissue at the cranial base and localized where a line perpendicular to the S-Ba line crosses the sphenoid bone; SN: anterior cranial base plane; Ba: Basion—The most inferoposterior point in the sagittal plane on the anterior rim of the foramen magnum—the tip of the posterior cranial base; S: Sella—The midpoint of sella; N: Nasion—The most anterior point of the frontonasal suture in the midsagittal plane; Pt: the most superior and posterior point of pterygomaxillary fissure; Go: gonion—The point at the intersection of lines tangent to the posterior border of the ramus; Gn: gnathion—The most anterior inferior point of the bony chin; Pog: pogonion—The most anterior point of the bony chin in the midsagittal plane; L1: Lower center incisor.

2.3.2 Imaging measurement

Scanned CBCT radiographs were processed using Mimics (Materialise NV, Belgium) on Samsung computer monitors (LF27T350FHEXXV, Korea). To isolate the airway space, the threshold value was set to a range of −1024 to −100 Hounsfield units. The pharyngeal airway volume was calculated by summing the maxilla and mandibular parts of the pharyngeal airway volume. Lateral cephalometric radiographs were analyzed using WEBCEPH software (version 1.5.0, Korea). Photos were obtained according to the manufacturer's recommended standard techniques and posture. The evaluation indicators were determined according to the illustrated figures and tables (Fig. 1, Ref. [24]; Figs. 2,3, Table 1).

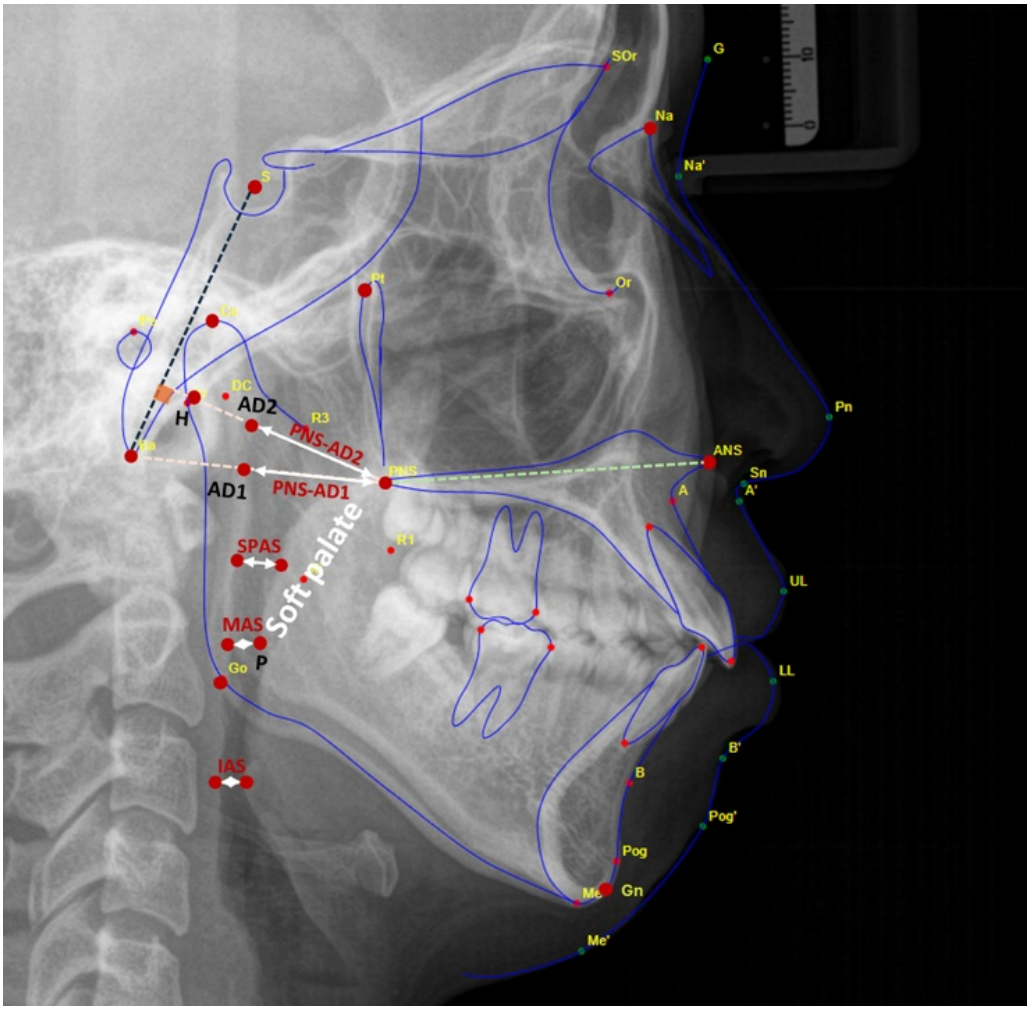

FIGURE 1. Limitations of airway analyses via lateral cephalometric radiography. PNS-AD2 (mm): the distance between PNS and AD2, which is a point on posterior pharyngeal wall intersecting the H-PNS line; PNS-AD1 (mm): the distance between PNS and AD1, a point on posterior pharyngeal wall intersecting the Ba-PNS line; SPAS (mm): the line parallel to the palatal plane between the midpoint of PNS and P and the posterior pharyngeal wall; MAS (mm): the line extending to the anterior and posterior pharyngeal walls from point P; IAS (mm): the line parallel to the palatal plane passing through the anteroinferior point of CV2 and the anterior pharyngeal wall. Hormion (H): the cephalometric point located near the adenoidal tissue at the cranial base and localized where a line perpendicular to the S-Ba line crosses the sphenoid bone. The variations of this point are minimal because it is located far away from growth sites (Table 1) [24].

2.3.3 The airway analyses via lateral cephalometric radiography

PNS-AD2 (mm): the distance between PNS and AD2, which is a point on posterior pharyngeal wall intersecting the H-PNS line: the line between PNS and H point; Hormion (H): the cephalometric point located near the adenoidal tissue at the cranial base and localized where a line perpendicular to the S-Ba line crosses the sphenoid bone. The variations of this point are minimal because it is located far away from growth sites.

PNS-AD1 (mm): the distance between PNS and AD1, a point on posterior pharyngeal wall intersecting the Ba-PNS line;

SPAS (mm): the line parallel to the palatal plane between the midpoint of PNS and P and the posterior pharyngeal wall;

MAS (mm): the line extending to the anterior and posterior pharyngeal walls from point P;

IAS (mm): the line parallel to the palatal plane passing through the anteroinferior point of CV2 and the anterior pharyngeal wall.

2.3.4 Craniofacial measurements via lateral cephalometric radiography

SNA (°): Angle between the line Sella-Nasion, and line Nasion-point A. This angle measures the position of the maxilla relative to the skull base;

SNB (°): Angle between the line point A—Nasion, and line point Nasion—point B. This angle measures the mandibular's position relative to the skull base;

ANB (°): Angle between line point A—the Nasion and line point B—Nasion, indicating the relationship between the maxilla and mandibular;

SN-GoGn (°): the angle between the SN plane and Steiner's mandibular plane (Go-Gn);

FMA (°): the angle between the Frankfort (FH) plane and

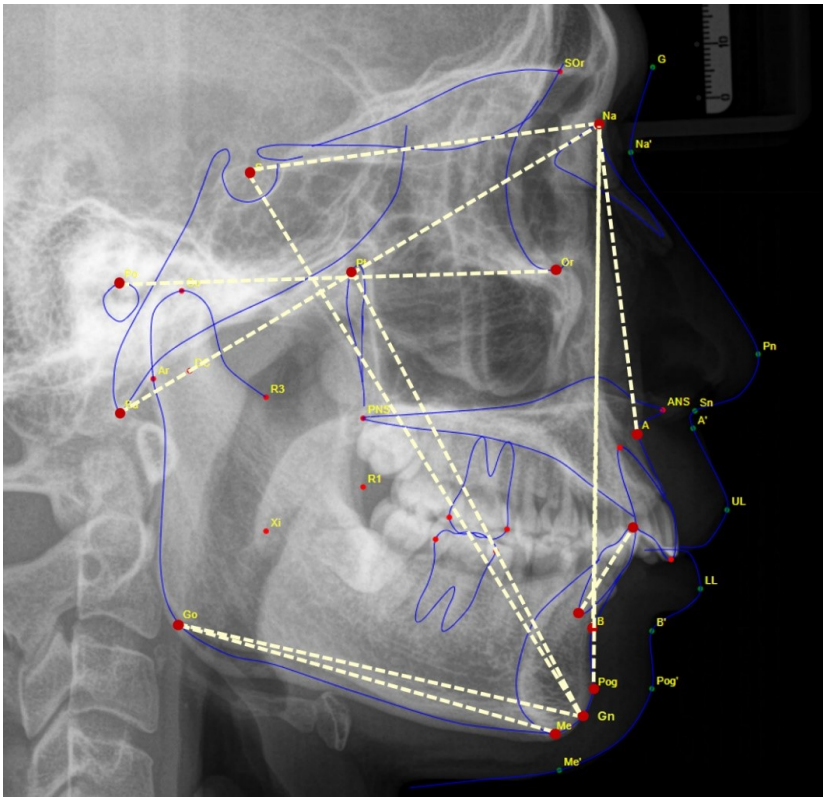

FIGURE 2. Craniofacial measurements via lateral cephalometric radiography. SNA (°): Angle between the line Sella-Nasion, and line Nasion-point A. This angle measures the position of the maxilla relative to the skull base; SNB (°): Angle between the line point A-Nasion, and line point Nasion-point B. This angle measures the mandibular's position relative to the skull base; ANB (°): Angle between line point A—the Nasion and line point B—Nasion, indicating the relationship between the maxilla and mandibular; SN-GoGn (°): the angle between the SN plane and Steiner's mandibular plane (Go-Gn); FMA (°): the angle between the Frankfort (FH) plane and Downs' mandibular plane (Go-Me). Facial axis (°): the angle between the Ba-N line and Pt-Gn line; Y-axis (°): the angle between the S-Gn and FH planes; Facial Angle (°): the angle between the FH plane and the N-Pog line; L-MP (°): the angle formed by the long axis of the mandibular incisor and the mandibular plane (Go-Me) (Table 1).

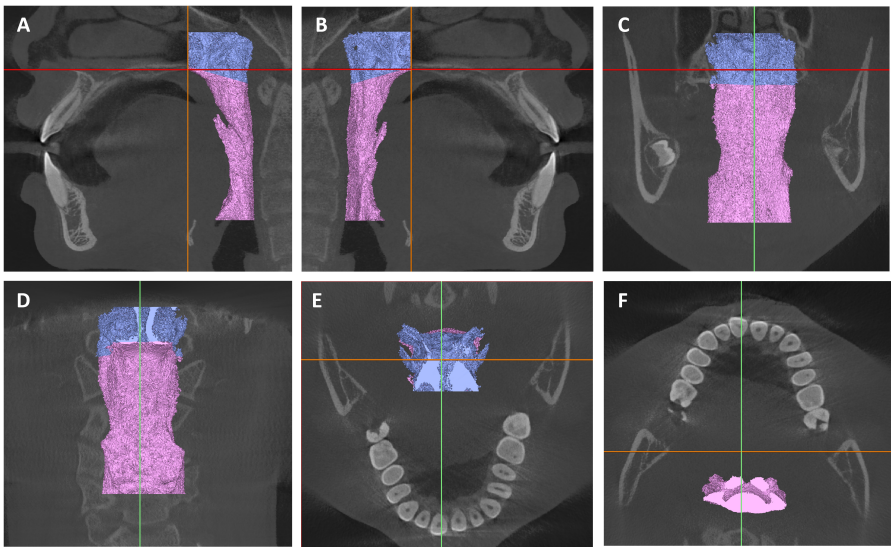

FIGURE 3. Three-dimensional image of the pharyngeal airway. (A) Left; (B) Right; (C) Anterior; (D) Posterior; (E) Superior; (F) Inferior. The upper airway extends from the nasal vestibule to the glottis, encompassing the nasal cavity, nasopharynx, oropharynx and hypopharynx. Airway Boundaries: the anterior region is defined by the hard palate, mandible and soft palate; the posterior pharyngeal wall, which stretches from the base of the skull to the level of the cervical vertebrae, borders the posterior region; superiorly, it is limited by the base of the skull and the nasal cavity; the inferior region extends to the level of the epiglottis.

Downs' mandibular plane (Go-Me);

Facial axis (°): the angle between the Ba-N line and Pt-Gn line;

Y-axis (°): the angle between the S-Gn and FH planes;

Facial Angle (°): the angle between the FH plane and the N-Pog line;

L1-MP (°): the angle formed by the long axis of the mandibular incisor and the mandibular plane (Go-Me).

2.3.5 Three-dimensional of the pharyngeal airway

The upper airway extends from the nasal vestibule to the glottis, encompassing the nasal cavity, nasopharynx, oropharynx and hypopharynx. Airway Boundaries: the anterior region is defined by the hard palate, mandible and soft palate; the posterior pharyngeal wall, which stretches from the base of the skull to the level of the cervical vertebrae, borders the posterior region; superiorly, it is limited by the base of the skull and the nasal cavity; the inferior region extends to the level of the epiglottis.

2.4 Statistical analysis

The collected figs and data were imported into Microsoft Excel 2020 (Microsoft Corporation, Redmond, WA, USA) and Google Drive. All radiographs were obtained by a dental imaging technician. The results were evaluated by comparing and reformatting anatomical structural components with different planes in 3D space to obtain the most appropriate image and then evaluating and measuring the related parameters. Statistical analyses were performed using SPSS (version 20.0; IBM Corp., Armonk, NY, USA). Analysis of variance (ANOVA) Test, Tukey's Test, Kruskal-Wallis Test, Dunn's Test and Pearson's correlation coefficients were used to analyze the data. Statistical significance was defined as $p \leq 0.05$.

3. Results

There were statistically significant differences between the skeletal CI, CII and CIII groups for the SNB, ANB, SN-GoGn, FMA, mandibular length, facial axis, Y-axis, facial angle and L1-MP. Conversely, the angles (SNA) and lower anterior facial height showed no significant differences. The mandibular length progressively decreased from skeletal CIII > skeletal CI > skeletal CII groups. However, there was a significant difference between skeletal CI and skeletal CII, and between skeletal CII and skeletal CIII (Table 2).

The lateral cephalometric analysis of airway dimensions showed that the PNS-AD2, SPAS and IAS measurements significantly differed between the CI, CII and CIII malocclusion

TABLE 2. Lateral cephalometric craniofacial measurements.

Skeletal pattern	Mean ± SD	*p*	Pairwise comparison	*p*
SNA (°)				
Class I	84.37 ± 2.78		Class I–Class II	0.218 (b)
Class II	85.81 ± 3.75	0.061 (a)	Class II–Class III	0.058 (b)
Class III	83.83 ± 4.04		Class III–Class I	0.798 (b)
SNB (°)				
Class I	82.26 ± 2.59		Class I–Class II	0.001** (b)
Class II	79.17 ± 3.78	<0.001*** (a)	Class II–Class III	<0.001*** (b)
Class III	81.31 ± 29.91		Class III–Class I	<0.001*** (b)
ANB (°)				
Class I	2.11 ± 0.99		Class I–Class II	<0.001*** (b)
Class II	6.63 ± 1.91	<0.001*** (a)	Class II–Class III	<0.001*** (b)
Class III	−2.60 ± 2.15		Class III–Class I	<0.001*** (b)
GnGo-SN (°)				
Class I	28.27 ± 3.50		Class I–Class II	<0.001*** (b)
Class II	33.71 ± 5.64	<0.001*** (a)	Class II–Class III	<0.001*** (b)
Class III	28.02 ± 5.68		Class III–Class I	0.976 (b)
FMA (°)				
Class I	23.02 ± 4.43		Class I–Class II	<0.001*** (b)
Class II	29.30 ± 6.05	<0.001*** (a)	Class II–Class III	0.669 (b)
Class III	24.10 ± 5.22		Class III–Class I	<0.001*** (b)
Mandibular length (mm)				
Class I	72.90 ± 4.47		Class I–Class II	<0.001*** (b)
Class II	68.00 ± 4.78	<0.001*** (a)	Class II–Class III	<0.001*** (b)
Class III	73.33 ± 4.41		Class III–Class I	0.921 (b)

TABLE 2. Continued.

Skeletal pattern	Mean ± SD	*p*	Pairwise comparison	*p*
Facial axis (°)				
Class I	87.82 ± 3.28		Class I–Class II	<0.001*** (b)
Class II	83.22 ± 4.16	<0.001*** (a)	Class II–Class III	<0.001*** (b)
Class III	90.43 ± 3.80		Class III–Class I	0.013* (b)
Y-axis (°)				
Class I	60.23 ± 2.44		Class I–Class II	<0.001*** (b)
Class II	63.35 ± 3.50	<0.001*** (a)	Class II–Class III	<0.001*** (b)
Class III	58.38 ± 2.85		Class III–Class I	0.029* (b)
Facial Angle (°)				
Class I	89.16 ± 1.78		Class I–Class II	<0.001*** (b)
Class II	85.50 ± 3.18	<0.001*** (a)	Class II–Class III	<0.001*** (b)
Class III	91.95 ± 3.21		Class III–Class I	<0.001*** (b)
L1-MP (°)				
Class I	96.51 ± 5.33		Class I–Class II	0.321 (b)
Class II	98.67 ± 5.78	<0.001*** (a)	Class II–Class III	<0.001*** (b)
Class III	85.34 ± 7.42		Class III–Class I	<0.001*** (b)
Lower Anterior Facial Height (LAFH) (mm)				
Class I	51.13		Class I–Class II	
Class II	56.04	0.766 (c)	Class II–Class III	Pairwise comparisons were not performed (d)
Class III	51.83		Class III–Class I	

(a) ANOVA Test; (b) Tukey's Test; (c) Kruskal-Wallis Test; (d) Dunn's Test.
**p < 0.05, **p < 0.01, ***p < 0.001.*
SNA (°): Angle between the line Sella-Nasion and line Nasion-point A. This angle measures the position of the maxilla relative to the skull base; SNB (°): Angle between the line point A—Nasion, and line point Nasion—point B. This angle measures the mandibular's position relative to the skull base; ANB (°): Angle between line point A—the Nasion and line point B—Nasion, indicating the relationship between the maxilla and mandibular; SN-GoGn (°): The angle between the SN plane and Steiner's mandibular plane (Go-Gn); FMA (°): The angle between the Frankfort (FH) plane and Downs' mandibular plane (Go-Me); Facial axis (°): The angle between the Ba-N line and Pt-Gn line; Y-axis (°): The angle between the S-Gn and FH planes; Facial Angle (°): The angle between the FH plane and the N-Pog line; L1-MP (°): The angle formed by the long axis of the mandibular incisor and the mandibular plane (Go-Me), LAFH: Lower Anterior Facial Height (mm): Distance measured from the (ANS) to the Menton (Me); Skeletal Class I (ANB angle between 0° and 4°), skeletal Class II (ANB angle ≥4°) and skeletal Class III (ANB angle <0°).

groups. Specifically, CIII exhibited the largest airway width, followed by CI and CII. However, comparing each skeletal group, there was a significant difference between skeletal CI and skeletal CII in PNS-AD2, between skeletal CII and skeletal CIII in SPAS, and between skeletal CII and skeletal CIII in IAS (Table 3).

The pharyngeal airway volume on CBCT radiographs was evaluated based on the nasopharynx, oropharynx and the total oropharyngeal volume. For the nasopharynx, we observed the largest volume in CIII, followed by CII and CIII groups, with significant differences between skeletal CI and skeletal CII, and between skeletal CI and skeletal CII. For the oropharynx, the volume also progressively decreased from CIII > CI > CII, with significant differences between skeletal CII and skeletal CIII. There was also a significant difference between skeletal CI and skeletal CII regarding airway volume. CIII had the most volume (27,237.66 ± 5699.12 mm^3), with CI having 26,372.73 ± 4577.11 mm^3, while Class II had the least volume (22,678.74 ± 4978.22 mm^3) with significant differences between skeletal CI and skeletal CII (Table 4).

There was a negative relationship between the airway parameters on lateral cephalometric radiographs and the airway volume on CBCT radiographs. This relationship was shown by the ANB and SN-GoGn angles, the FMA and the Y-axis as they exhibited a positive correlation with mandibular body length, the facial axis and the facial angle (Table 5). There was also a positive correlation between the airway parameters on lateral cephalometric radiographs and airway volume on CBCT radiographs (Tables 6,7,8,9).

4. Discussion

Currently, aesthetic concerns are being increasingly emphasized by patients, with achieving a flawless appearance being

TABLE 3. Pharyngeal airway dimensions on lateral cephalometric radiographs.

Skeletal pattern	Mean Rank	*p*	Pairwise comparison	*p*
PNS-AD1 (mm)				
Class I	51.16		Class I–Class II	Pairwise comparisons were not performed (b)
Class II	52.34	0.827 (a)	Class II–Class III	
Class III	55.50		Class III–Class I	
PNS-AD2 (mm)				
Class I	20.98 ± 2.61		Class I–Class II	0.004** (d)
Class II	18.61 ± 3.52	0.006** (c)	Class II–Class III	0.054 (d)
Class III	20.35 ± 3.16		Class III–Class I	0.603 (d)
SPAS (mm)				
Class I	12.32 ± 3.03		Class I–Class II	0.112 (d)
Class II	11.04 ± 2.39	0.010* (c)	Class II–Class III	0.008** (d)
Class III	12.96 ± 2.41		Class III–Class I	0.562 (d)
MAS (mm)				
Class I	10.81 ± 3.04		Class I–Class II	0.711 (d)
Class II	10.33 ± 2.28	0.137 (c)	Class II–Class III	0.118 (d)
Class III	11.54 ± 2.18		Class III–Class I	0.451 (d)
IAS (mm)				
Class I	11.78 ± 3.23		Class I–Class II	0.2 (d)
Class II	10.44 ± 3.48	0.050* (c)	Class II–Class III	0.044*(d)
Class III	12.41 ± 3.42		Class III–Class I	0.716 (d)

(a) ANOVA Test; (b) Tukey's Test; (c) Kruskal-Wallis Test; (d) Dunn's Test.
**p < 0.05, **p < 0.01.*
PNS-AD2 (mm): the distance between PNS and AD2, which is a point on posterior pharyngeal wall intersecting the H-PNS line; (Hormion (H): the cephalometric point located near the adenoidal tissue at the cranial base and localized where a line perpendicular to the S-Ba line crosses the sphenoid bone. The variations of this point are minimal because it is located far away from growth sites); PNS-AD1 (mm): The distance between PNS and AD1, a point on posterior pharyngeal wall intersecting the Ba-PNS line; SPAS (mm): The line parallel to the palatal plane between the midpoint of PNS and P and the posterior pharyngeal wall; MAS (mm): The line extending to the anterior and posterior pharyngeal walls from point P; IAS (mm): The line parallel to the palatal plane passing through the anteroinferior point of CV2 and the anterior pharyngeal wall; Skeletal Class I (ANB angle between 0° and 4°), skeletal Class II (ANB angle ≥4°) and skeletal Class III (ANB angle <0°).

TABLE 4. Pharyngeal airway volume on cone bean computed tomography radiographs.

Skeletal pattern	Mean ± SD	*p*	Pairwise comparison	*p*
NP (mm^3)				
Class I	9966.69 ± 2275.68		Class I–Class II	0.005** (b)
Class II	8169.07 ± 2410.13	0.001** (a)	Class II–Class III	0.002** (b)
Class III	10,149.14 ± 2338.08		Class III–Class I	0.943 (b)
OP (mm^3)				
Class I	16,406.03 ± 3589.04		Class I–Class II	0.120 (b)
Class II	14,516.46 ± 3955.68	0.023* (a)	Class II–Class III	0.022* (b)
Class III	17,072.77 ± 4336.80		Class III–Class I	0.763 (b)
TP (mm^3)				
Class I	26,372.73 ± 4577.11		Class I–Class II	0.009** (b)
Class II	22,678.74 ± 4978.22	0.001** (a)	Class II–Class III	0.001** (b)
Class III	27,237.66 ± 5699.12		Class III–Class I	0.759 (b)

(a) ANOVA Test; (b) Tukey's Test.
**p < 0.05, **p < 0.01.*
NP: Nasopharynx (mm^3): The region superior to the plane passes through the two points of the posterior nasal spine (PNS) on both sides and the first cervical vertebra (C1); OP: Oropharynx (mm^3): The region inferior to the plane passes through the two points of the posterior nasal spine (PNS) on both sides and the first cervical vertebra (C1); TP: Total pharynx (mm^3): The volume that includes both the nasopharynx and oropharynx; Skeletal Class I (ANB angle between 0° and 4°), skeletal Class II (ANB angle ≥4°) and skeletal Class III (ANB angle <0°).

TABLE 5. Correlation between pharyngeal airway parameters on cone beam computed tomography and lateral cephalometric radiographs with craniofacial measurements.

Total	SNA	SNB	ANB	GnGo-SN	FMA	Mandibular length	Facial axis	Y-axis	LAFH	Facial angle	L1-MP
NP											
Pearson correlation	−0.215	0.068	−0.284	−0.165	−0.206	0.197	0.121	−0.093	0.094	0.161	−0.114
Sig. (2-tailed)	0.027	0.492	0.003	0.093	0.035	0.044	0.218	0.343	0.340	0.101	0.249
OP											
Pearson correlation	−0.053	0.061	−0.338	−0.362	−0.348	0.411	0.430	−0.347	0.012	0.320	−0.109
Sig. (2-tailed)	0.592	0.536	<0.001	<0.001	<0.001	<0.001	<0.001	<0.001	0.903	0.001	0.269
TP											
Pearson correlation	−0.138	0.077	−0.385	−0.350	−0.358	0.402	0.381	−0.305	0.052	0.316	−0.134
Sig. (2-tailed)	0.161	0.432	<0.001	<0.001	<0.001	<0.001	<0.001	0.002	0.596	0.001	0.175
PNS-AD2											
Pearson correlation	−0.064	0.177	−0.237	−0.244	−0.283	0.272	0.163	−0.197	0.019	0.240	−0.001
Sig. (2-tailed)	0.514	0.070	0.015	0.012	0.003	0.005	0.097	0.044	0.845	0.014	0.989
PNS-AD1											
Pearson correlation	−0.118	0.047	−0.120	−0.114	−0.211	0.203	0.144	−0.167	0.049	0.122	0.006
Sig. (2-tailed)	0.231	0.633	0.222	0.248	0.031	0.038	0.143	0.089	0.619	0.215	0.949
SPAS											
Pearson correlation	−0.072	0.070	−0.353	−0.231	−0.270	0.344	0.440	−0.384	<0.001	0.368	−0.270
Sig. (2-tailed)	0.462	0.480	<0.001	0.018	0.005	<0.001	<0.001	<0.001	0.996	<0.001	0.005
MAS											
Pearson correlation	−0.060	−0.006	−0.253	−0.131	−0.167	0.331	0.314	−0.239	0.088	0.261	−0.190
Sig. (2-tailed)	0.542	0.950	0.009	0.183	0.088	0.001	0.001	0.014	0.370	0.007	0.053
IAS											
Pearson correlation	0.084	0.171	−0.252	−0.186	−0.168	0.349	0.291	−0.223	0.087	0.309	−0.138
Sig. (2-tailed)	0.396	0.081	0.009	0.058	0.086	<0.001	0.003	0.022	0.379	0.001	0.162

Pearson correlation coefficient.

NP: Nasopharynx (mm^3): The region superior to the plane passes through the two points of the posterior nasal spine (PNS) on both sides and the first cervical vertebra (C1); OP: Oropharynx (mm^3): The region inferior to the plane passes through the two points of the posterior nasal spine (PNS) on both sides and the first cervical vertebra (C1); TP: Total pharynx (mm^3): The volume that includes both the nasopharynx and oropharynx; PNS-AD2 (mm): The distance between PNS and AD2, which is a point on posterior pharyngeal wall intersecting the H-PNS line; (Hormion (H): The cephalometric point located near the adenoidal tissue at the cranial base and localized where a line perpendicular to the S-Ba line crosses the sphenoid bone. The variations of this point are minimal because it is located far away from growth sites); PNS-AD1 (mm): The distance between PNS and AD1, a point on posterior pharyngeal wall intersecting the Ba-PNS line; SPAS (mm): The line parallel to the palatal plane between the midpoint of PNS and P and the posterior pharyngeal wall; MAS (mm): The line extending to the anterior and posterior pharyngeal walls from point P; IAS (mm): The line parallel to the palatal plane passing through the anteroinferior point of CV2 and the anterior pharyngeal wall; SNA (°): Angle between the line Sella-Nasion, and line Nasion-point A. This angle measures the position of the maxilla relative to the skull base; SNB (°): Angle between the line point A—Nasion and line point Nasion—point B. This angle measures the mandibular's position relative to the skull base; ANB (°): Angle between line point A—the Nasion and line point B—Nasion, indicating the relationship between the maxilla and mandibular; SN-GoGn (°): The angle between the SN plane and Steiner's mandibular plane (Go-Gn); FMA (°): The angle between the Frankfort (FH) plane and Downs' mandibular plane (Go-Me); Facial axis (°): The angle between the Ba-N line and Pt-Gn line; Y-axis (°): The angle between the S-Gn and FH planes; Facial Angle (°): The angle between the FH plane and the N-Pog line; L1-MP (°): The angle formed by the long axis of the mandibular incisor and the mandibular plane (Go-Me); LAFH: Lower Anterior Facial Height (mm): Distance measured from the (ANS) to the Menton (Me).

TABLE 6. Correlation between pharyngeal airway volume and craniofacial measurements in skeletal Class I malocclusion.

Skeletal Class I	SNA	SNB	ANB	GnGo-SN	FMA	Mandibular length	Facial axis	Y-axis	LAFH	Facial angle	L1-MP
NP											
Pearson correlation	−0.342	−0.379	0.029	0.210	0.062	−0.091	−0.278	0.272	0.087	−0.239	−0.080
Sig. (2-tailed)	0.044	0.025	0.870	0.226	0.722	0.603	0.106	0.114	0.621	0.166	0.649
OP											
Pearson Correlation	−0.130	0.131	−0.304	−0.123	−0.007	0.082	0.325	−0.145	−0.115	0.063	0.086
Sig. (2-tailed)	0.940	0.453	0.076	0.483	0.969	0.641	0.057	0.404	0.510	0.717	0.625
TP											
Pearson Correlation	−0.160	−0.086	−0.224	0.008	0.026	0.019	0.116	0.021	−0.047	−0.069	0.027
Sig. (2-tailed)	0.360	0.624	0.196	0.962	0.884	0.915	0.505	0.904	0.787	0.693	0.876
PNS-AD2											
Pearson Correlation	−0.010	−0.078	0.178	0.047	0.067	−0.027	−0.072	0.060	0.006	−0.102	0.041
Sig. (2-tailed)	0.956	0.656	0.307	0.787	0.704	0.877	0.680	0.730	0.974	0.560	0.813
PNS-AD1											
Pearson Correlation	−0.066	0.012	−0.215	−0.146	−0.117	0.268	0.147	<0.001	0.243	0.042	0.086
Sig. (2-tailed)	0.705	0.947	0.215	0.402	0.503	0.120	0.399	0.999	0.159	0.813	0.625
SPAS											
Pearson Correlation	0.120	0.148	−0.049	−0.084	−0.034	0.219	0.314	−0.093	0.143	0.126	−0.082
Sig. (2-tailed)	0.492	0.397	0.780	0.633	0.846	0.207	0.067	0.597	0.413	0.471	0.640
MAS											
Pearson Correlation	0.134	0.185	−0.107	−0.048	−0.003	0.357	0.268	−0.103	0.230	0.156	−0.027
Sig. (2-tailed)	0.442	0.286	0.540	0.782	0.988	0.035	0.119	0.557	0.185	0.369	0.879
IAS											
Pearson Correlation	0.082	0.132	−0.113	−0.002	−0.013	0.312	0.191	−0.088	0.145	0.095	0.056
Sig. (2-tailed)	0.638	0.450	0.518	0.991	0.939	0.068	0.272	0.615	0.407	0.588	0.751

Pearson correlation coefficient.

NP: Nasopharynx (mm^3): The region superior to the plane passes through the two points of the posterior nasal spine (PNS) on both sides and the first cervical vertebra (C1); OP: Oropharynx (mm^3): The region inferior to the plane passes through the two points of the posterior nasal spine (PNS) on both sides and the first cervical vertebra (C1); TP: Total pharynx (mm^3): The volume that includes both the nasopharynx and oropharynx; PNS-AD2 (mm): The distance between PNS and AD2, which is a point on posterior pharyngeal wall intersecting the H-PNS line; (Hormion (H): The cephalometric point located near the adenoidal tissue at the cranial base and localized where a line perpendicular to the S-Ba line crosses the sphenoid bone. The variations of this point are minimal because it is located far away from growth sites); PNS-AD1 (mm): The distance between PNS and AD1, a point on posterior pharyngeal wall intersecting the Ba-PNS line; SPAS (mm): The line parallel to the palatal plane between the midpoint of PNS and P and the posterior pharyngeal wall; MAS (mm): The line extending to the anterior and posterior pharyngeal walls from point P; IAS (mm): The line parallel to the palatal plane passing through the anteroinferior point of CV2 and the anterior pharyngeal wall; SNA (°): Angle between the line Sella-Nasion, and line Nasion-point A. This angle measures the position of the maxilla relative to the skull base; SNB (°): Angle between the line point A—Nasion and line point Nasion—point B. This angle measures the mandibular's position relative to the skull base; ANB (°): Angle between line point A—the Nasion and line point B—Nasion, indicating the relationship between the maxilla and mandibular; SN-GoGn (°): The angle between the SN plane and Steiner's mandibular plane (Go-Gn); FMA (°): The angle between the Frankfort (FH) plane and Downs' mandibular plane (Go-Me); Facial axis (°): The angle between the Ba-N line and Pt-Gn line; Y-axis (°): The angle between the S-Gn and FH planes; Facial Angle (°): The angle between the FH plane and the N-Pog line; L1-MP (°): The angle formed by the long axis of the mandibular incisor and the mandibular plane (Go-Me); LAFH: Lower Anterior Facial Height (mm): Distance measured from the (ANS) to the Menton (Me).

TABLE 7. Correlation between pharyngeal airway volume and craniofacial measurements in skeletal class II malocclusion.

Skeletal class II	SNA	SNB	ANB	GnGo-SN	FMA	Mandibular length	Facial axis	Y-axis	LAFH	Facial angle	L1-MP
NP											
Pearson correlation	−0.218	−0.273	0.112	0.071	−0.015	0.032	−0.244	0.216	0.232	−0.198	0.169
Sig. (2-tailed)	0.209	0.113	0.521	0.687	0.932	0.854	0.159	0.212	0.181	0.255	0.333
OP											
Pearson correlation	−0.035	0.038	−0.143	−0.296	−0.328	0.534	0.293	−0.199	0.158	0.131	0.125
Sig. (2-tailed)	0.841	0.830	0.411	0.084	0.055	0.001	0.088	0.253	0.366	0.454	0.473
TP											
Pearson Correlation	−0.132	−0.102	−0.058	−0.200	−0.266	0.440	0.114	−0.051	0.293	0.008	0.182
Sig. (2-tailed)	0.450	0.561	0.742	0.248	0.122	0.008	0.514	0.769	0.166	0.966	0.295
PNS-AD2											
Pearson Correlation	−0.167	−0.114	−0.102	−0.035	−0.158	0.008	−0.118	−0.008	0.004	0.013	0.217
Sig. (2-tailed)	0.336	0.513	0.560	0.841	0.366	0.965	0.499	0.961	0.982	0.939	0.211
PNS-AD1											
Pearson Correlation	−0.201	−0.180	−0.039	−0.005	−0.225	0.199	0.011	−0.138	0.024	0.092	0.206
Sig. (2-tailed)	0.246	0.301	0.824	0.977	0.193	0.251	0.952	0.428	0.889	0.599	0.236
SPAS											
Pearson Correlation	−0.143	0.016	−0.311	−0.095	−0.255	0.439	0.295	−0.323	−0.039	0.277	−0.110
Sig. (2-tailed)	0.412	0.930	0.069	0.586	0.139	0.008	0.085	0.058	0.824	0.107	0.529
MAS											
Pearson Correlation	−0.069	0.003	−0.140	−0.087	−0.207	0.406	0.225	−0.156	0.008	0.201	−0.151
Sig. (2-tailed)	0.694	0.987	0.423	0.620	0.232	0.016	0.194	0.369	0.963	0.247	0.387
IAS											
Pearson Correlation	0.276	0.365	−0.180	−0.178	−0.134	0.482	0.224	−0.107	0.212	0.323	0.006
Sig. (2-tailed)	0.109	0.031	0.300	0.306	0.443	0.003	0.196	0.540	0.221	0.059	0.971

Pearson correlation coefficient.

NP: Nasopharynx (mm^3): The region superior to the plane passes through the two points of the posterior nasal spine (PNS) on both sides and the first cervical vertebra (C1); OP: Oropharynx (mm^3): The region inferior to the plane passes through the two points of the posterior nasal spine (PNS) on both sides and the first cervical vertebra (C1); TP: Total pharynx (mm^3): The volume that includes both the nasopharynx and oropharynx; PNS-AD2 (mm): The distance between PNS and AD2, which is a point on posterior pharyngeal wall intersecting the H-PNS line; (Hormion (H): The cephalometric point located near the adenoidal tissue at the cranial base and localized where a line perpendicular to the S-Ba line crosses the sphenoid bone. The variations of this point are minimal because it is located far away from growth sites); PNS-AD1 (mm): The distance between PNS and AD1, a point on posterior pharyngeal wall intersecting the Ba-PNS line; SPAS (mm): The line parallel to the palatal plane between the midpoint of PNS and P and the posterior pharyngeal wall; MAS (mm): The line extending to the anterior and posterior pharyngeal walls from point P; IAS (mm): The line parallel to the palatal plane passing through the anteroinferior point of CV2 and the anterior pharyngeal wall; SNA (°): Angle between the line Sella-Nasion, and line Nasion-point A. This angle measures the position of the maxilla relative to the skull base; SNB (°): Angle between the line point A—Nasion and line point Nasion—point B. This angle measures the mandibular's position relative to the skull base; ANB (°): Angle between line point A—the Nasion and line point B—Nasion, indicating the relationship between the maxilla and mandibular; SN-GoGn (°): The angle between the SN plane and Steiner's mandibular plane (Go-Gn); FMA (°): The angle between the Frankfort (FH) plane and Downs' mandibular plane (Go-Me); Facial axis (°): The angle between the Ba-N line and Pt-Gn line; Y-axis (°): The angle between the S-Gn and FH planes; Facial Angle (°): The angle between the FH plane and the N-Pog line; L1-MP (°): The angle formed by the long axis of the mandibular incisor and the mandibular plane (Go-Me); LAFH: Lower Anterior Facial Height (mm): Distance measured from the (ANS) to the Menton (Me).

TABLE 8. Correlation between pharyngeal airway volume and craniofacial measurements in skeletal class III malocclusion.

Skeletal class III	SNA	SNB	ANB	GnGo-SN	FMA	Mandibular length	Facial axis	Y-axis	LAFH	Facial angle	L1-MP
NP											
Pearson correlation	0.048	0.148	−0.048	−0.187	−0.191	0.152	0.118	−0.071	0.042	0.050	0.135
Sig. (2-tailed)	0.786	0.396	0.786	0.281	0.271	0.387	0.500	0.686	0.809	0.775	0.440
OP											
Pearson correlation	0.045	0.060	−0.353	−0.359	−0.411	0.364	0.434	−0.382	0.024	0.334	−0.014
Sig. (2-tailed)	0.799	0.732	0.037	0.034	0.014	0.032	0.009	0.024	0.891	0.050	0.937
TP											
Pearson correlation	0.055	0.107	−0.290	−0.355	−0.398	0.346	0.382	−0.323	0.035	0.277	0.049
Sig. (2-tailed)	0.755	0.540	0.091	0.036	0.018	0.042	0.023	0.059	0.841	0.107	0.781
PNS-AD2											
Pearson correlation	0.174	0.300	−0.201	−0.304	−0.322	0.486	0.209	−0.236	0.105	0.314	0.083
Sig. (2-tailed)	0.319	0.080	0.247	0.075	0.060	0.003	0.228	0.172	0.548	0.066	0.635
PNS-AD1											
Pearson correlation	0.022	0.147	0.060	−0.195	−0.296	0.069	0.227	−0.274	−0.145	0.047	0.084
Sig. (2-tailed)	0.901	0.401	0.733	0.261	0.084	0.695	0.190	0.112	0.406	0.790	0.632
SPAS											
Pearson correlation	0.013	0.086	−0.311	−0.187	−0.254	0.088	0.450	−0.442	−0.087	0.327	−0.231
Sig. (2-tailed)	0.941	0.622	0.069	0.283	0.140	0.613	0.007	0.008	0.621	0.055	0.183
MAS											
Pearson correlation	−0.121	−0.053	−0.333	−0.068	−0.167	0.089	0.305	−0.265	0.021	0.221	−0.094
Sig. (2-tailed)	0.489	0.761	0.050	0.697	0.337	0.610	0.075	0.124	0.906	0.203	0.589
IAS											
Pearson correlation	0.070	0.222	−0.030	−0.061	−0.074	0.029	0.145	−0.130	−0.052	0.160	−0.043
Sig. (2-tailed)	0.691	0.200	0.863	0.726	0.673	0.871	0.406	0.458	0.767	0.359	0.807

Pearson correlation coefficient.

NP: Nasopharynx (mm^3): The region superior to the plane passes through the two points of the posterior nasal spine (PNS) on both sides and the first cervical vertebra (C1); OP: Oropharynx (mm^3): The region inferior to the plane passes through the two points of the posterior nasal spine (PNS) on both sides and the first cervical vertebra (C1); TP: Total pharynx (mm^3): The volume that includes both the nasopharynx and oropharynx; PNS-AD2 (mm): The distance between PNS and AD2, which is a point on posterior pharyngeal wall intersecting the H-PNS line; (Hormion (H): The cephalometric point located near the adenoidal tissue at the cranial base and localized where a line perpendicular to the S-Ba line crosses the sphenoid bone. The variations of this point are minimal because it is located far away from growth sites); PNS-AD1 (mm): The distance between PNS and AD1, a point on posterior pharyngeal wall intersecting the Ba-PNS line; SPAS (mm): The line parallel to the palatal plane between the midpoint of PNS and P and the posterior pharyngeal wall; MAS (mm): The line extending to the anterior and posterior pharyngeal walls from point P; IAS (mm): The line parallel to the palatal plane passing through the anteroinferior point of CV2 and the anterior pharyngeal wall; SNA (°): Angle between the line Sella-Nasion, and line Nasion-point A. This angle measures the position of the maxilla relative to the skull base; SNB (°): Angle between the line point A—Nasion and line point Nasion—point B. This angle measures the mandibular's position relative to the skull base; ANB (°): Angle between line point A—the Nasion and line point B—Nasion, indicating the relationship between the maxilla and mandibular; SN-GoGn (°): The angle between the SN plane and Steiner's mandibular plane (Go-Gn); FMA (°): The angle between the Frankfort (FH) plane and Downs' mandibular plane (Go-Me); Facial axis (°): The angle between the Ba-N line and Pt-Gn line; Y-axis (°): The angle between the S-Gn and FH planes; Facial Angle (°): The angle between the FH plane and the N-Pog line; L1-MP (°): The angle formed by the long axis of the mandibular incisor and the mandibular plane (Go-Me); LAFH: Lower Anterior Facial Height (mm): Distance measured from the (ANS) to the Menton (Me).

TABLE 9. Correlation Between airway dimensions on lateral cephalometric and cone beam computed tomography radiographs.

Skeletal pattern		PNS-AD2	PNS-AD1	SPAS	MAS	IAS
NP						
Class I	Pearson correlation	0.312	0.403	0.164	0.263	0.070
	Sig. (2-tailed)	0.068	0.016	0.348	0.127	0.689
Class II	Pearson Correlation	0.617	0.617	0.124	0.167	−0.144
	Sig. (2-tailed)	<0.001	<0.001	0.479	0.337	0.409
Class III	Pearson Correlation	0.573	0.615	0.301	0.236	0.154
	Sig. (2-tailed)	<0.001	<0.001	0.079	0.172	0.376
Total	Pearson Correlation	0.596	0.533	0.273	0.263	0.104
	Sig. (2-tailed)	<0.001	<0.001	0.005	0.007	0.289
OP						
Class I	Pearson Correlation	0.027	0.393	0.372	0.382	0.291
	Sig. (2-tailed)	0.876	0.020	0.028	0.024	0.130
Class II	Pearson Correlation	0.704	0.395	0.571	0.516	0.324
	Sig. (2-tailed)	0.673	0.019	<0.001	0.002	0.058
Class III	Pearson Correlation	0.168	0.288	0.561	0.572	0.529
	Sig. (2-tailed)	0.335	0.093	<0.001	<0.001	0.001
Total	Pearson Correlation	0.171	0.368	0.529	0.494	0.420
	Sig. (2-tailed)	0.081	<0.001	<0.001	<0.001	<0.001
TP						
Class I	Pearson correlation	0.177	0.509	0.373	0.430	0.240
	Sig. (2-tailed)	0.310	0.002	0.027	0.010	0.165
Class II	Pearson Correlation	0.386	0.611	0.512	0.490	0.187
	Sig. (2-tailed)	0.022	<0.001	0.002	0.003	0.281
Class III	Pearson Correlation	0.367	0.476	0.550	0.531	0.529
	Sig. (2-tailed)	0.030	0.004	0.001	0.001	0.005
Total	Pearson correlation	0.403	0.521	0.522	0.491	0.362
	Sig. (2-tailed)	<0.001	<0.001	<0.001	<0.001	<0.001

Pearson correlation coefficient.
NP: Nasopharynx (mm^3): The region superior to the plane passes through the two points of the posterior nasal spine (PNS) on both sides and the first cervical vertebra (C1); OP: Oropharynx (mm^3): The region inferior to the plane passes through the two points of the posterior nasal spine (PNS) on both sides and the first cervical vertebra (C1); TP: Total pharynx (mm^3): The volume that includes both the nasopharynx and oropharynx; PNS-AD2 (mm): The distance between PNS and AD2, which is a point on posterior pharyngeal wall intersecting the H-PNS line; (Hormion (H): The cephalometric point located near the adenoidal tissue at the cranial base and localized where a line perpendicular to the S-Ba line crosses the sphenoid bone. The variations of this point are minimal because it is located far away from growth sites): PNS-AD1 (mm): The distance between PNS and AD1, a point on posterior pharyngeal wall intersecting the Ba-PNS line; SPAS (mm): The line parallel to the palatal plane between the midpoint of PNS and P and the posterior pharyngeal wall; MAS (mm): The line extending to the anterior and posterior pharyngeal walls from point P; IAS (mm): The line parallel to the palatal plane passing through the anteroinferior point of CV2 and the anterior pharyngeal wall; Skeletal Class I (ANB angle between 0° and 4°), skeletal Class II (ANB angle ≥4°) and skeletal Class III (ANB angle <0°).

a central focus. As a result, the number of patients seeking consultations and desiring orthodontic and facial skeletal corrections has risen. Moreover, epidemiological studies conducted across different populations and ethnic groups have indicated that the prevalence of malocclusion and the demand for orthognathic treatment are on the rise. Ishiguro's study highlighted a correlation between craniofacial structural shape and the patency of the airway [25]. Moss famously stated, "Function decides form" a concept that has strongly influenced current perspectives in orthognathic surgery and orthodontics. For example, patients who breathe through their mouths tend to exhibit a characteristic facial morphology. Conversely, facial morphology also affects function. Hakan EI and Juan Martin Palomo, in their study on airway dimensions across different craniofacial patterns, found that the oropharyngeal airway size was smallest in CII skeletal malocclusion patients, followed by CI, with the largest airway observed in CIII patients [26]. Therefore, failing to understand the oropharyngeal airway dimensions in patients with different types of malocclusion during orthognathic treatment can pose a risk to the patency of the airway and overall respiratory function.

Lateral cephalometric radiographs are basic screening tools that offer several advantages, such as low cost, minimal radiation exposure and reliable measurement data. As a result, these films are widely used in diagnosing and orthodontically correcting dental issues, as well as assessing the oropharyngeal airway dimensions in patients with CII skeletal malocclusion, which helps orthodontists develop individualized treatment plans. However, a primary limitation of lateral cephalometric radiographs is that they only evaluate the airway in the anteroposterior dimension. Therefore, to obtain a more comprehensive and accurate assessment of airway dimensions, CBCT provides the most reliable and effective imaging [27].

To better understand which factors of malocclusion may be related to changes in the maxilla airway, we evaluated the differences in craniofacial characteristics among the patient groups. These included correlations between the maxilla and mandibular jaw (ANB), mandibular length (Go-Me), mandibular position (SNB) and the growth direction of the mandible (SN-GoGn and FMA).

Regarding the mandibular body length, assessing the correlation between mandibular length and airway dimensions, a positive correlation was observed. This finding supports the notion that mandibular length may be related to oropharyngeal airway size, which is consistent with a study by Muto *et al.* [28], who demonstrated that craniofacial abnormalities, including retrognathism, a short mandibular body and downward rotation of the mandible can lead to a reduction in airway size. Additionally, a study by Yu-Chuan Tseng *et al.* [29] indicated that airway dimensions decrease as the position of the mandible moves posteriorly. However, our study did not find a significant correlation between mandibular position (SNB) and airway size.

Clinical studies have demonstrated a relationship between the craniofacial system and the airway across different skeletal patterns. When comparing various growth patterns, significant differences in airway width and volume have been observed. Our study, conducted on different malocclusion groups classified according to the ANB angle, found an inverse correlation between the ANB angle and oropharyngeal airway dimensions. As the ANB angle increased, the airway size decreased. CII subjects, having the highest ANB angle, exhibited the smallest airway dimensions. Conversely, CIII patients with the lowest ANB angle had the largest airway dimensions. These findings are consistent with those of other studies [29, 30].

Different skeletal growth patterns may develop due to various factors, such as the growth of the maxilla and mandible, the maxillary-mandibular dental relationship, tooth eruption and tongue function. It is known that most individuals with a vertical growth pattern tend to experience simultaneous maxilla airway obstruction, often accompanied by symptoms such as snoring, daytime sleepiness and mouth breathing [31]. Therefore, the relationship between growth patterns and the airway must be assessed to create better orthodontic treatment plans. Our results indicate that airway dimensions are reduced in individuals with a vertical growth pattern. Specifically, as the SN-GoGn angle and FMA increase, the airway size decreases and *vice versa*. Thus, in clinical situations, it is advisable to avoid downward and posterior rotation of the mandible to prevent further reduction in airway volume.

Trenouth and Timms proposed a theory linking mandibular length to the oropharyngeal airway. They hypothesized that increased mandibular length resulted in the anterior displacement of the genioglossus and geniohyoid muscle attachments, thereby widening the pharyngeal airway [32]. One study found that the mandibular length (Go-Me) was shorter in people with skeletal Class II patterns compared to Class III patterns. That study also showed a link between Go-Me and the volume of the pharynx. The results showed that there were differences in the size of the pharyngeal airway between skeletal Class II and III malocclusions, which may support Trenouth and Timms's theory [32, 33].

Only the nasopharynx and oropharynx of the upper airway were the focus of this research. However, the literature provides substantial evidence that individuals with skeletal disorders affect all three sections of the upper airway (nasopharynx, oropharynx and hypopharynx). Therefore, future studies should also assess the hypopharynx. Further studies should expand upon these results by integrating more thorough airway evaluations. This may include using imaging modalities such as cone-beam computed tomography (CBCT) or magnetic resonance imaging (MRI), which see the hypopharynx and the remainder of the upper airway in three dimensions. Incorporating dynamic evaluations, such as sleep studies, might be beneficial to understand how these structural variations influence function.

Incorporating dynamic evaluations and broadening the range of airway measurements enables researchers to get deeper insights into the interplay between skeletal malocclusion, airway dimensions, and the progression of obstructive sleep apnea.

This study has several limitations that should be considered when interpreting the findings. Firstly, the cross-sectional design of the study prevents us from establishing causal relationships between skeletal malocclusions and upper airway dimensions. Secondly, the sample was limited to Vietnamese children, which may reduce the generalizability of the results to other populations with different ethnic or cultural charac-

teristics. Lastly, the study did not account for other factors such as environmental influences, respiratory conditions or genetic predispositions, which could impact the upper airway dimensions independently of skeletal malocclusions.

5. Conclusions

Craniofacial morphology can influence nasal respiratory function and the maxillary airway. There was a strong correlation between airway volume and skeletal patterns. Airway dimensions were significantly reduced in skeletal Class II malocclusion patients with a high ANB angle, retrognathic mandible and vertical growth pattern. Clinicians should exercise caution when performing mandibular retrusion in skeletal Class II patients to avoid worsening airway obstruction. It is essential to determine the most suitable treatment for each patient and avoid methods that may further reduce airway size in individuals who already have a tendency toward smaller airway dimensions. This is especially crucial for preventing the onset of obstructive sleep apnea in patients. Furthermore, this study highlights the importance of lateral cephalometric radiographs in evaluating the airway.

AVAILABILITY OF DATA AND MATERIALS

The data that support the findings of this study are available from the corresponding author, upon reasonable request.

AUTHOR CONTRIBUTIONS

LNL and TTNN—collected and analyzed the data. LNL, TTNN, LTT, TTHT and PTTN—designed the research study and wrote the manuscript. LNL, TTNN, LTT, TTHT, PTTN and KVPL—reviewed and edited the manuscript. All authors read and approved the final version of the manuscript.

ETHICS APPROVAL AND CONSENT TO PARTICIPATE

This retrospective study was conducted according to the guidelines of the Declaration of Helsinki and all procedures performed were following the Ethics Committee of the University of Medicine and Pharmacy of Can Tho University in Biomedical Research No: 23.002/PCT-HDDD. Consent was obtained from the parents or guardians for the use of all images of children in the manuscript.

ACKNOWLEDGMENT

The authors thank the technical support provided by the Faculty of Odonto and Stomatology, Can Tho University of Medicine and Pharmacy and Can Tho University of Medicine and Pharmacy Hospital, Can Tho City, Vietnam.

FUNDING

This research received no external funding.

CONFLICT OF INTEREST

The authors declare no conflict of interest.

REFERENCES

[1] Pop SI, Procopciuc A, Arsintescu B, Mihai M, Loredana M, Radu VP, *et al*. Three-dimensional assessment of upper airway volume and morphology in patients with different sagittal skeletal patterns. Diagnostics. 2024; 14: 903.

[2] Erten O, Yılmaz B. Three-dimensional imaging in orthodontics. Turkish Journal of Orthodontics. 2018; 31: 86.

[3] Öztekin A, Öztekin C. Images download cite share favorites permissions research article: observational study the evolution of pemphigus publications: a bibliometric analysis with research trends and global productivity. Medicine. 2024; 103: e38047.

[4] Maken P, Gupta A. 2D-to-3D: a review for computational 3D image reconstruction from X-ray images. Archives of Computational Methods in Engineering. 2023; 30: 85–114.

[5] Altheer C, Papageorgiou SN, Antonarakis GS, Papadopoulou A. Do patients with different craniofacial patterns have differences in upper airway volume? A systematic review with network meta-analysis. European Journal of Orthodontics. 2024; 46: cjae010.

[6] Mouhanna-Fattal C, Papadopoulos M, Bouserhal J, Tauk A, Bassil-Nassif N, Athanasiou AJIO. Evaluation of upper airway volume and craniofacial volumetric structures in obstructive sleep apnoea adults: a descriptive CBCT study. International Orthodontics. 2019; 17: 678–686.

[7] Steegman R, Hogeveen F, Schoeman A, Ren Y, Surgery M. Cone beam computed tomography volumetric airway changes after orthognathic surgery: a systematic review. International Journal of Oral and Maxillofacial Surgery. 2023; 52: 60–71.

[8] Zimmerman JN, Lee J, Pliska B. Reliability of upper pharyngeal airway assessment using dental CBCT: a systematic review. European Journal of Orthodontics. 2017; 39: 489–496.

[9] Di Carlo G, Polimeni A, Melsen B, Cattaneo PMJO. The relationship between upper airways and craniofacial morphology studied in 3D: a CBCT study. Orthodontics & Craniofacial Research. 2015; 18: 1–11.

[10] Habumugisha J, Mohamed AS, Cheng B, Liu L, Zou R, Wang F. Analysis of maxillary arch morphology and its relationship with upper airway in mouth breathing subjects with different sagittal growth patterns. Journal of Stomatology Oral and Maxillofacial Surgery. 2023; 124: 101386.

[11] Dodda KK, Prasad SERV, Kanuru RK, Nalluri S, Mittapalli R, Raghavendra. Diagnostic features of Angle's class II div 2 malocclusion. Journal of International Society of Preventive and Community Dentistry. 2015; 5: 513–517.

[12] Sfondrini MF, Gallo S, Pascadopoli M, Gandini P, Roncoroni C, Scribante AJDJ. Upper airway dimensions among different skeletal malocclusions: a retrospective observational study by cephalometric analysis. Journal of Dentistry. 2024; 12: 12.

[13] Alswairki H, Alam M, Rahman S, Alsuwailem R, Alanazi S. Upper airway changes in diverse orthodontic looms: a systematic review and meta-analysis. Applied Sciences. 2022; 12: 916.

[14] Lombardo G, Vena F, Negri P, Pagano S, Barilotti C, Paglia L, *et al*. Worldwide prevalence of malocclusion in the different stages of dentition: a systematic review and meta-analysis. European Journal of Paediatric Dentistry. 2020; 21: 115–122.

[15] Rodrigues J, Evangelopoulos E, Anagnostopoulos I, Sachdev N, Ismail A, Samsudin R, *et al*. Impact of class II and class III skeletal malocclusion on pharyngeal airway dimensions: a systematic literature review and meta-analysis. Heliyon. 2024; 10: e27284.

[16] Abdelkarim A. Cone-beam computed tomography in orthodontics. Dentistry Journal. 2019; 7: 89.

[17] Asquith J, Gillgrass T, Mossey P. Three-dimensional imaging of orthodontic models: a pilot study. European Journal of Orthodontics. 2007; 29: 517–522.

[18] Gupta S, Tandon P, Singh GP, Shastri D. Comparative assessment of cephalometric with its analogous photographic variables. National Journal of Maxillofacial Surgery. 2022; 13: 99–107.

[19] Tsolakis IA, Tsolakis AI, Elshebiny T, Matthaios S, Palomo JM.

Comparing a fully automated cephalometric tracing method to a manual tracing method for orthodontic diagnosis. Journal of Clinical Medicine. 2022; 11: 6854.

[20] Baldini B, Cavagnetto D, Baselli G, Sforza C, Tartaglia GM. Cephalometric measurements performed on CBCT and reconstructed lateral cephalograms: a cross-sectional study providing a quantitative approach of differences and bias. BMC Oral Health. 2022; 22: 98.

[21] Van Minh H, Khuong DQL, Tran TA, Do HP, Watson F, Lobstein T. Childhood overweight and obesity in Vietnam: a landscape analysis of the extent and risk factors. Inquiry. 2023; 60: 00469580231154651.

[22] Van de Perck E, Van Hoorenbeeck K, Verhulst S, Saldien V, Vanderveken OM, Boudewyns A. Effect of body weight on upper airway findings and treatment outcome in children with obstructive sleep apnea. Sleep Medicine. 2021; 79: 19–28.

[23] Colceriu-Şimon IM, Băciuţ M, Ştiufiuc RI, Aghiorghiesei A, Ţărmure V, Lenghel M, *et al*. Clinical indications and radiation doses of cone beam computed tomography in orthodontics. Medical and Pharmaceutical Reports. 2019; 92: 346.

[24] Atik E, Coskuner H, Kocadereli I. Dentoskeletal and airway effects of the X-Bow appliance versus removable functional appliances (Frankel-2 and Trainer) in prepubertal class II division 1 malocclusion patients. Australasian Orthodontic Journal. 2017; 33: 3–13.

[25] Ishiguro K, Kobayashi T, Kitamura N, Saito CJOS. Relationship between severity of sleep-disordered breathing and craniofacial morphology in Japanese male patients. Oral Surgery Oral Medicine Oral Pathology Oral Radiology and Endodontics. 2009; 107: 343–349.

[26] El H, Palomo J. Airway volume for different dentofacial skeletal patterns. American Journal of Orthodontics and Dentofacial Orthopedics. 2011; 139: e511–e521.

[27] Ghoneima A, Kula K. Accuracy and reliability of cone-beam computed tomography for airway volume analysis. European Journal of Orthodontics. 2013; 35: 256–261.

[28] Muto T, Yamazaki A, Takeda S. A cephalometric evaluation of the pharyngeal airway space in patients with mandibular retrognathia and prognathia, and normal subjects. International Journal of Oral and Maxillofacial Surgery. 2008; 37: 228–231.

[29] Tseng YC, Tsai FC, Chou ST, Hsu CY, Cheng JH, Chen CM. Evaluation of pharyngeal airway volume for different dentofacial skeletal patterns using cone-beam computed tomography. Journal of Dental Sciences. 2021; 16: 51–57.

[30] Maheshwari S, Anjum A, Suting GS, Farhan S, Khan A. Evaluation of changes in tongue pressure with twin-block appliance therapy in growing class II div 1 malocclusion. An *in vivo* study. Journal of Orthodontic Science. 2023; 12: 69.

[31] Firwana A, Wang H, Sun L, Wang J, Zhang W. Relationship of the airway size to the mandible distance in Chinese skeletal class I and class II adults with normal vertical facial pattern. Indian Journal of Dental Research. 2019; 30: 368–374.

[32] Trenouth MJ, Timms DJ. Relationship of the functional oropharynx to craniofacial morphology. Angle Orthodontist. 1999; 69: 419–423.

[33] Habumugisha J, Nakamura M, Kono K, Uchida K, Konko M, Izawa T, *et al*. Novel prediction models for pharyngeal-airway volume based on the cranial-base and midsagittal cross-sectional area of the airway in the pharyngeal region: a cephalometric and magnetic resonance imaging study. Orthodontics & Craniofacial Research. 2024; 27: 394–402.

How to cite this article: Lam Nguyen Le, Trinh Thi Ngoc Nguyen, Loc Truong Tan, Tranh Thi Huyen Trinh, Phung Thi Thanh Nguyen, Khanh Vu Phuong Le. Upper airway dimensions with different skeletal malocclusions? A cross-sectional study in Vietnamese children. Journal of Clinical Pediatric Dentistry. 2025; 49(3): 149-164. doi: 10.22514/jocpd.2025.062.